



A case study on the rockfall assessment and stability analysis along Lengpui-Aizawl highway, Mizoram, India

Sahil Sardana¹ · Pushpendra Sharma² · Amit Kumar Verma³ · Trilok Nath Singh⁴

Received: 23 May 2020 / Accepted: 31 October 2020 / Published online: 2 January 2021
© Saudi Society for Geosciences 2021

Abstract

Roadways are the lifeline for any city, especially in hilly regions. The increase in population and road constructions has led to the destabilization of the slopes resulting in mass movement. Anisotropic rockmass, whose behaviour is largely dependent on the planes of weakness, was simulated using *3DEC*. The three-dimensional discontinuum modelling technique provides the most rigorous analysis of the failure process and deformation in the anisotropic rock. However, due to the limited capacity of the software, it is impossible to include all the discontinuities implicitly in numerical simulation. This paper provides a methodology for the application of Ubiquitous-Joint models on a field scale to include the anisotropic behaviour of rockmass. After identifying the failure-prone area using rigorous *3DEC* slope stability analysis, rockfall analysis was also carried out to identify the maximum run-out, bounce height and total kinetic energy of falling rock blocks in the same section of the slope. *3DEC* results show the maximum total displacement of 2.6 cm with a maximum velocity of 0.25 m/s, which confirms the instability in the slope. The rockfall simulation reveals that the falling rock blocks can hit the vehicle on the roadway with the kinetic energy of 58.5 kJ that makes this roadway unsafe.

Keywords Road cut slopes · Ubiquitous-joint model · *3DEC* · Rockfall · Aizawl · Slope stability

Introduction

The strength of the rockmass mainly depends on two factors, intact rock strength and the presence of discontinuities (joints, faults, foliation, and bedding). Deformation and failure process in jointed rockmass can be simulated using an equivalent continuum rockmass model or discontinuum model. Later, the

model can be simulated using *3DEC* (three-dimensional distinct element code). *3DEC* has the capability to model the behaviour of the individual rigid or deformable block formed by the intersection of two or more different joints based on a variety of block and joint constitutive models. Joints are considered as boundary conditions between intact rock blocks; large displacement along the joints and rotation of the intact rock blocks are simulated. On a large scale (field scale) where the joint spacing is very low and the number of joints is very high, it is very difficult to solve the mathematical model in the practical timeline by including all the joints due to the limited computation capability of work stations. In such scenarios, the continuum-based Ubiquitous-Joint constitutive model was adapted to consider the effect of discontinuities on rockmass strength (Sainsbury and Sainsbury 2017). This model accounts for the presence of the orientation of weakness (weak plane) in a Mohr-Coulomb model. Failure criteria on any given plane of weakness consist of a composite Mohr-Coulomb failure envelope with tension cut-off. The state of stress in the plastic region is updated by considering a non-associated flow rule for shear failure criteria and an associated flow rule for tension failure criteria. The associated length or spacing of the weakness plane is considered negligible in the Ubiquitous-

Responsible Editor: Zeynal Abiddin Erguler

✉ Amit Kumar Verma
akverma.min@iitbhu.ac.in

¹ Department of Mining Engineering, Indian Institute of Technology (Indian School of Mines), Dhanbad, Jharkhand 826004, India

² Department of Civil Engineering, Lassonde School of Engineering, York University, Toronto, Canada

³ Department of Mining Engineering, Indian Institute of Technology (Banaras Hindu University), Varanasi, Uttar Pradesh 221005, India

⁴ Department of Earth Science, Indian Institute of Technology Bombay, Mumbai, Maharashtra 400076, India

Joint model, while the effect of weak plane direction is simulated. The rigidity of bedding planes can also be neglected; the ubiquitous joint behaviour may be misrepresented if the calibrated material properties are not used. The properties for the numerical model can be determined at a laboratory scale by calibrating experimental results with the small-scale numerical model test. The limitation of the Ubiquitous-Joint model is that they do not consider the effect of joint spacing, persistence and joint stiffness into the numerical model. Subiquitous constitutive model simulates strain softening/hardening behaviour of the joint as well as intact rock block with calibrated properties in the post-failure region, together with Ubiquitous-Joint model which uses a bilinear Mohr-Coulomb failure envelope. For both Ubiquitous and Subiquitous models, failure is detected first based on the Mohr-Coulomb criteria for the matrix; here, properties of the rock matrix are determined using anisotropic strength calibration of the rock mass. The evaluated stress state is updated based on the given failure criteria and plastic strain evolution rule. The new stresses are used for failure detection on the plane of weakness and updated accordingly. The properties of calibrated intact rock block can be determined using anisotropic strength calibration. Anisotropic strength calibration should be carried out to evaluate the joint set, spacing and direction which will have a major effect on the rock mass strength. Joint sets that cause minimum strength of the rockmass will only be applied and evaluate the field performance of the calibrated Subiquitous model at a large scale. The stability of an anisotropic slope is analysed using *3DEC*. Total displacement and velocity contours are used to decide the unstable areas in the slope. Further, the rockfall analysis can be used in the unstable zones to identify the parameters such as bounce height, run-out distance, velocity and kinetic energy of the fall-out rock blocks.

Rockfall is very common in hilly regions; the high energies and velocities associated with the falling rock blocks result in damages of vehicles and infrastructures and fatalities. Rainfall (Wei et al. 2014), freeze-thaw (Blikra and Christiansen 2014) and earthquakes (Valagussa et al. 2014) trigger the rockfall activity in the mountainous region. The Aizawl region witnessed heavy rainfall during the monsoon season, which is one of the primary causes of rockfall along this highway. Root penetration and unplanned excavation are other parameters which affect the rockfall activity (Wieczorek and Jäger 1996). Basically, four types of motions (i.e. roll, fall, bounce and slide) occur when a rock block separates from the slope surface. Kinetic energy during fall motion is higher than other types of rockfall motion. The probability of fall motion is more in vertical or sub-vertical slopes which makes the rockfall assessment necessary in this region (Verma and Singh 2010). Rockfall analysis identifies the parameters such as bounce height, run-out distance, velocity and kinetic energy of the falling rock block. These parameters are further used for the proper selection of protective measurements such as

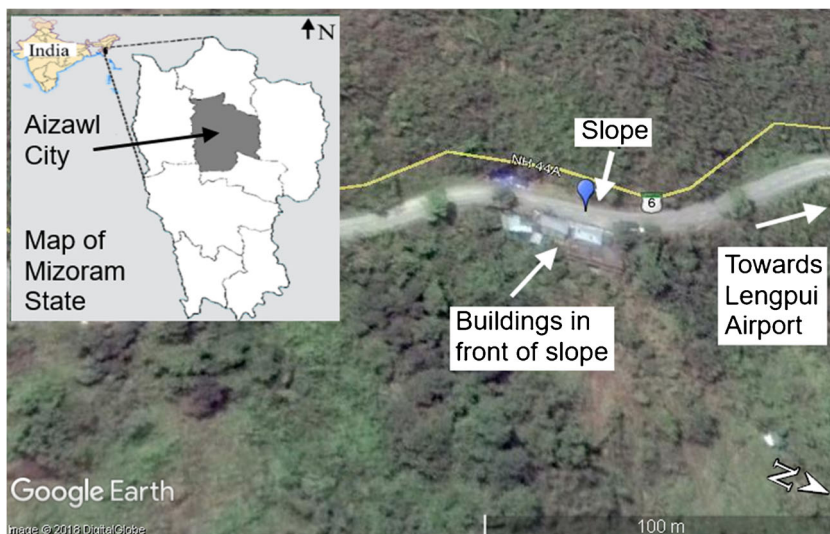
ditches, barriers, retaining walls and many more (Wang et al. 2012). Many researchers have conducted rockfall studies (Singh et al. 2013; Ansari et al. 2016; Chiliza and Hingston 2018; Verma et al. 2018) and slope stability assessment (Singh and Verma 2007; Ferrari et al. 2014; Sarkar et al. 2016; Tang et al. 2017; Verma et al. 2016; Warren et al. 2016; Kumar et al. 2018, Sardana et al. 2019a, b) using different techniques. The presence of buildings on the opposite side of the studied slope makes it necessary to carry out the slope stability analysis as well as the rockfall analysis.

Area of investigation

The studied slope is located along the NH-44A between Lengpui and Aizawl in the northeast region of India. Coordinates of the studied slope are 23° 46' 52.95" N and 92° 40' 21.42" E. The location of the slope comes under toposheet no. 83D/15, 83D/16 and 84A/10 of Survey of India. It is approximately 17 km away from Lengpui Airport towards Aizawl City (Fig. 1). An extensive survey was carried out at the studied slope to measure geological and other parameters. Three types of joint sets—joint J1 (90/140), joint J2 (65/078) and bedding (32/268)—were measured in the field. The dip and dip-direction of the slope were measured to 70/267. Joint spacing at the site was varied from 90 to 150 cm for joint J1, 40–90 cm for joint J2 and 10–20 cm for bedding J3. The persistence of joints was found up to 10 m for joint J1, up to 5 m for joint J2 and 5–10 m for bedding J3. The roughness and weathering of the joints were slight to moderate for all three joint sets. A soft infilling material was also observed between the joints in the slope. The height and length of the slope were measured to be 15 m and 43 m, respectively, with a roadway width of 6 m. During the site investigation, three to four residential buildings were found on the opposite side of the slope face. The slope is composed of sandstone, whereas mostly sandstone-shale intercalation was observed in this region. The Lengpui-Aizawl highway (NH-44A) is the only highway that connects the city to the airport. Slopes along this highway have a history of rockfall, and this region is marked as a rockfall-prone area by the PWD.

The region comes under Bhuban dispositions of the Surma group (Kesari 2011). This group of rocks embraces alternate beds of shale, siltstone, sandstone and mudstone of diverse thicknesses. Sandstones are hard, compact and stable, whereas shale beds are brittle as compared with sandstone. They include bands of micaceous-feldspathic and weathered sandstone (Lallianthanga and Lalbiakmawia 2013). An arenaceous and argillaceous batch of rocks lies in relatively upper and lower grounds, respectively. Reconnaissance traversing from Aizawl to Champhai resulted in the identification of a Barail batch of rocks in and around the Champhai subdivision, Aizawl district and Bhuban in the west.

Fig. 1 Modified Google image of the studied slope along the Lengpui-Aizawl highway



Methodology

This paper focuses on numerical stability analysis as well as the rockfall stability for the road cut slope along highway NH-44A. The methodology used in this paper is shown in Fig. 2. A site investigation was carried out to find out the geometrical and geological parameters of the slope. The rock samples of nearly rectangular-shaped blocks were collected from the freshly exposed surface of the slope as well as the failed rock blocks that were dislodged from the slope to determine the geo-mechanical properties of the rock and coefficient of restitution (CoR). Three-dimensional numerical modelling was carried out using the field observations and the block properties calculated from the laboratory. Initially, anisotropic strength calibration at a laboratory scale was carried out using a numerical model to evaluate the properties of equivalent rockmass blocks and implicit joints. The unstable section in the slope was identified by the 3D numerical modelling. Further, rockfall modelling was carried out to analyse the bounce height, velocity, kinetic energy and the run-out distance of falling rock block. The input parameters of the rockfall model such as CoR, the shape of geometry and the size of falling blocks were taken from the field observation. The unstable section of the slope identified in the numerical modelling was considered as the rockfall initiation point.

3DEC modelling

3DEC is a three-dimensional tool based on the distinct element method and can be used for the discontinuum numerical modelling of the jointed rock slopes. The model analysed the failure in the rock slope to evaluate the influence of joints and faults on the excavation. It is suitable for the study of the potential mode of failure due to the presence of discontinuous features. The properties of the joint can be assigned independently to individual

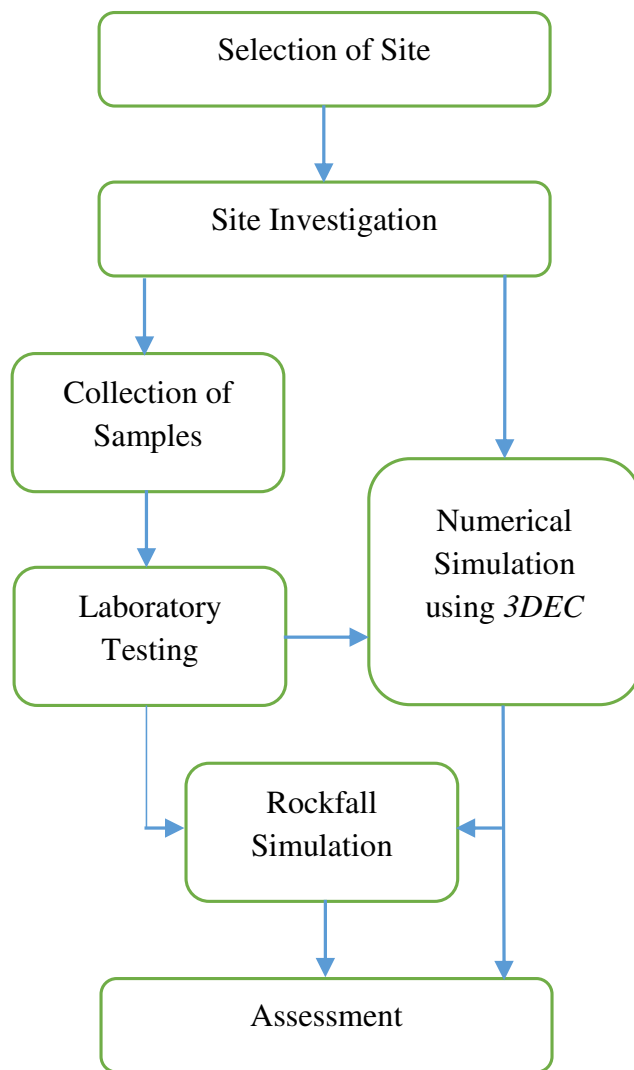


Fig. 2 A flowchart showing methodology

Table 1 Intact rock properties determined in the laboratory for numerical simulations

Rock properties	Min.	Max.	Mean	Standard deviation	Standard error
Uniaxial compressive strength (MPa)	76.69	98.46	88.36	8.69	4.34
Brazilian tensile strength (MPa)	1.76	3.82	2.8	0.79	0.39
Young's modulus, E (GPa)			25.49		
Poisson's ratio, ν			0.3		
Cohesion, c (MPa)			5.8		
Angle of internal friction, ϕ			35.8		

blocks or sets of discontinuity in a model. The model works on Coulomb slip criteria which assign the different characteristics such as elastic stiffness, frictional, cohesive and tensile strengths and dilation to a joint. Blocks in *3DEC* simulation can be either rigid or deformable. The material models for deformable blocks range from the 'null' block material (excavations) to the shear yielding models (strain-hardening/softening behaviour). *3DEC* was originally developed for the stability analysis of the jointed rock slopes. Nowadays, it is frequently used in the studies and research related to mining engineering, including both static and dynamic analyses of underground mines.

In this study, *3DEC* is used to analyse the stability of a three-dimensional model of studied rock slope on NH-44A. The slope contains three joint sets with spacing varying from 20 to 150 cm. It is difficult to include all the joint sets in the numerical model due to the computational intensity of the software. Therefore, based on the field observation, the spacing of joint sets which have a major effect on the stability of slope was selected as 3 m. The properties of the rock block matrix formed between these joint sets were evaluated using anisotropic strength calibration analysis. Subiquitous joint model (mohr coulomb + implicit joint + strain softening) was used to simulate the constitutive behaviour of rock mass matrix and implicit joints. The behaviour of the rock mass matrix between the joint sets was simulated using Ubiquitous-Joint constitutive model with strain softening. The anisotropic strength calibration was carried out on a 6 m uniaxial compressive sample numerically. The strength of the lab-scale model was evaluated using 3D discontinuum analysis and compared with the subiquitous joint model. The calibrated properties of the rock block matrix from the lab-scale numerical model was used for the simulation of the field-scale model. There were some assumptions made in the calibration process of the subiquitous model; for example, the behaviour from the discontinuum model was assumed to represent the actual behaviour. The observed strength of the bedding plane was assumed to represent the maximum strength of the ubiquitous joint in the continuum matrix. The length and stiffness of the ubiquitous

joint were neglected in the numerical model. To accompany the effect of persistence and stiffness of the joints not included implicitly in the numerical model, calibrated properties were used for the rock block matrix determined from the anisotropic strength analysis from the discontinuum model. The softening behaviour of the rock block matrix and implicit joints were calibrated from the lab-scale models. The rate of softening for both rock matrix and joint were selected based on the recommendations by Sainsbury and Sainsbury (2017). For simplicity, it was assumed that cohesion and tension for rock matrix and joints soften to zero in the post-failure region.

Rockfall modelling

Rocfall program from Rocscience (2016) was used for the assessment of rockfall. It is a two-dimensional statistical analysis tool for the rockfall risk assessment of the slopes. Slope geometry, slope material, rockfall initiation point and shape and size of the rock blocks are the primary input parameters that are used in the rockfall assessment. A detailed survey was carried out at the studied slope to observe and calculate the parameters that affect the rockfall event. Slope geometry was drawn to represent the actual slope profile. During the survey, a number of fallen rock blocks were observed near the slope. The dimensions of these rock blocks were measured to calculate their masses. The analysis in the Rocfall program is based on either lumped mass or rigid body approach. In the former approach, each rock block is considered as a very small spherical particle (i.e. only mass is considered; size of the rock block is not considered), whereas the latter approach considered the shape and size of the rock block depending on its mass. The analysis carried out in this paper is based on lumped mass formulation. The major output parameters that can be analysed from Rocfall are trajectories, bounce height, velocity and kinetic energy of falling rock block at any point. These output parameters further assist in the design of the size, capacity and location of the rockfall barriers.

Table 2 Explicit joint properties used in the numerical model

Property	Spacing	Joint normal stiffness	Joint shear stiffness	Cohesion	Friction angle
Value	3	9.82	3.11	0–0.1	32
Unit	m	GPa/m	GPa/m	MPa	°

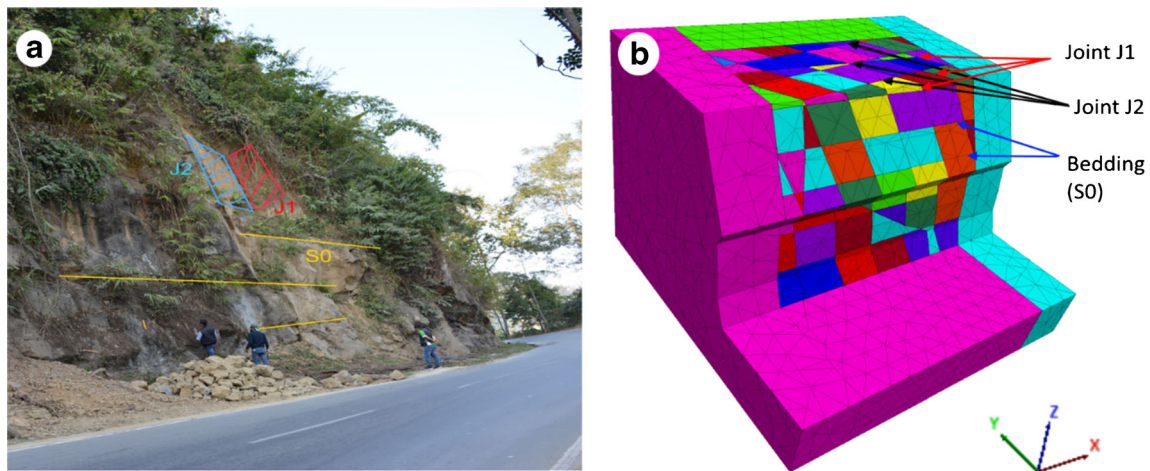


Fig. 3 a Photograph of studied slope showing joints (J1 and J2) and bedding (S0); b three-dimensional geometry of studied slope with joint mapping

Three-dimensional numerical simulation

A three-dimensional numerical analysis was performed using *3DEC* (Itasca 2016). The actual geometry of the road cut slope is given in Fig. 3a, and corresponding geometry used in the numerical model is shown in Fig. 3b. Discontinuum numerical methods have the capability to simulate joints explicitly in the anisotropic rockmass. In the numerical model, joint sets J1, J2 and J3 are simulated explicitly with spacing greater than the actual spacing in the field. Mohr-Coulomb slip with residual strength failure criteria was adopted in the numerical model. The intact properties of the rock were determined in the laboratory and are reported in Table 1. The properties of the rockmass were estimated using the empirical formulae based on parameters evaluated from the laboratory and field investigations (UCS, tensile strength; geological strength index, GSI). Further, these rockmass properties were used to estimate the normal and shear stiffness of the joint (Eqs. 1, 2). The joint properties used in the numerical analysis are provided in Table 2. The friction angle for the discontinuity was determined from field observation, for instance, surface roughness and alteration as suggested by Kulhawy (1975) and Barton (1976). The value of cohesion along the joint has a major effect on the strength of rockmass. Therefore, the critical value of cohesion is required to simulate the field

behaviour of the rockmass. In the numerical model, a range of values of cohesion had been chosen to decide the critical value. The values of cohesion were varied between 100 and 0 kPa, and the final value is adjusted in such a manner that the field behaviour is matched.

$$k_n = \frac{E_i E_m}{L(E_i - E_m)}, \tag{1}$$

$$k_s = \frac{G_i G_m}{L(G_i - G_m)} \tag{2}$$

where E_m = rock mass modulus, E_i = intact rock modulus, k_n = joint normal stiffness, G_m = rock mass shear modulus, G_i = intact rock shear modulus, k_s = joint shear stiffness and L = mean joint spacing.

Anisotropic strength calibration was carried out by simulating a large scale (i.e. 6 m) compression test to evaluate properties of rockmass. The compression test was simulated using *3DEC*. The spacing of the bedding plane was selected as 0.2 m, and moreover, the spacing for joint sets J1 and J2 is selected in such a way that the average block volume within the sample is 0.1 m³, which is consistent with an observed average GSI of 49 (Cai et al. 2007). The properties of intact rock block and explicit joints used in the calibration test are

Table 3 Properties of the matrix and implicit joints used in the Subiquitous numerical model based on anisotropic strength calibration

Rockmass matrix properties	Value	Unit	Implicit joint properties	Value (J1)	Unit
Density	2700	kg/m ³	Friction angle	24	°
Bulk modulus	4.32	GPa	Cohesion	0.01	MPa
Shear modulus	2.84	GPa	Tensile strength	0	MPa
Cohesion	1.2	MPa	ϵ_{crit}^{ps}	0.021	%
Friction angle	33	Degree			
Tensile strength	0.28	MPa			
ϵ_{crit}^{ps}	0.021	%			

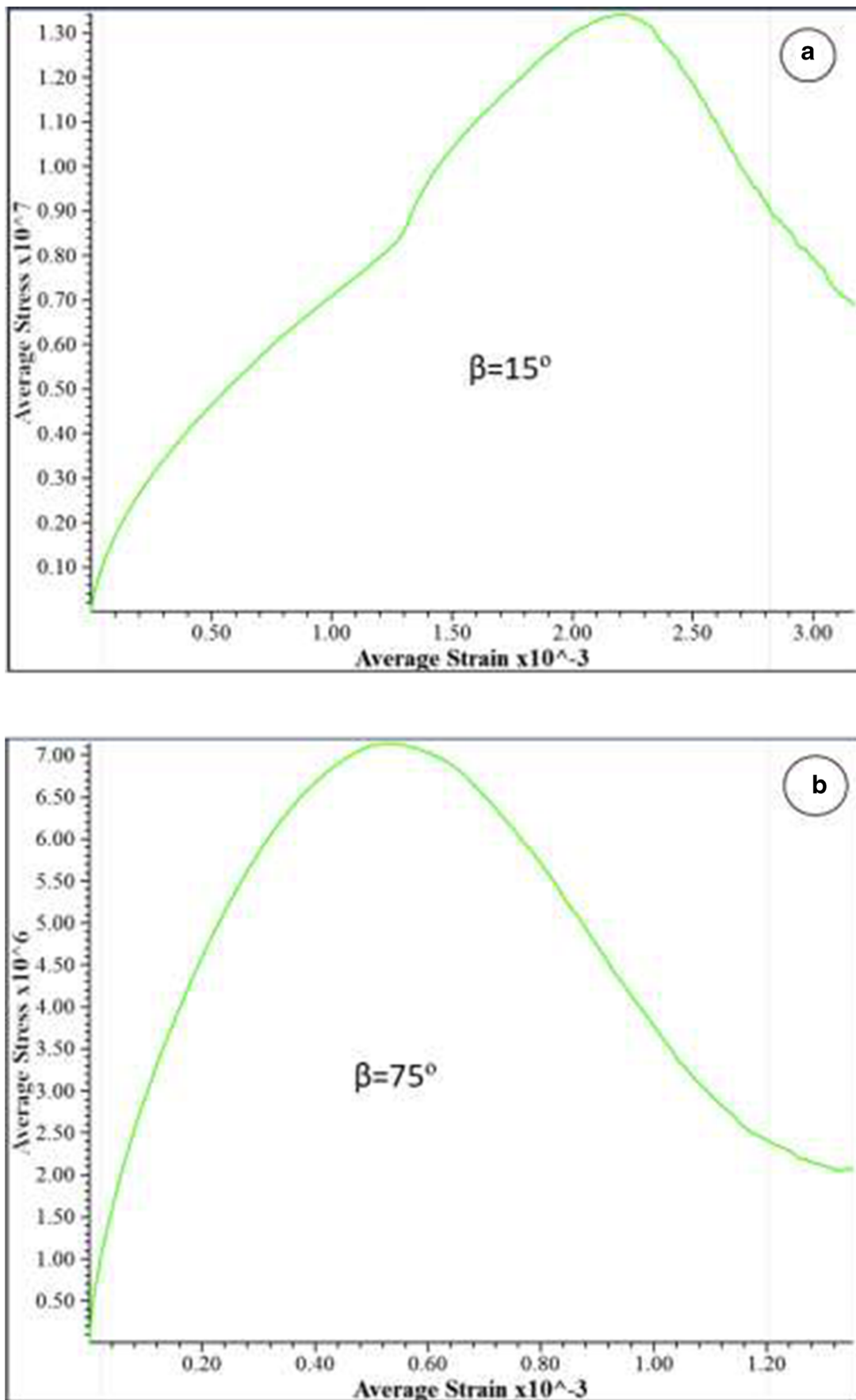
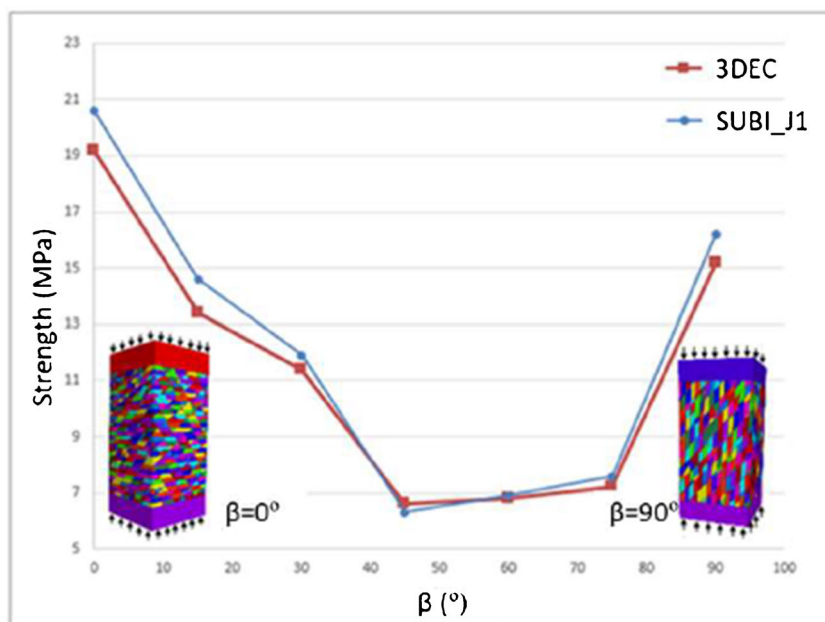


Fig. 4 Stress-strain response of the compression test for different orientation of the bedding plane viz. (a) $\beta = 15^\circ$ and (b) $\beta = 75^\circ$

Fig. 5 Comparison between the strength of the calibration sample evaluated from actual joint spacing and Subiquitous joint model for rockmass



given in Tables 1 and 2. The stress-strain response of the compression test for different orientations of the bedding plane viz. $\beta = 15^\circ$ and $\beta = 75^\circ$ is shown in Fig. 4a, b. A comparison between the strength of the calibration sample evaluated from the actual joint spacing and Subiquitous joint model for rockmass is shown in Fig. 5. The calibrated properties used in the numerical model for rockmass are given in Table 3. The deformation modulus was taken as 20% of the modulus measured in the laboratory, whereas the cohesion is decreased by 50% of the intact value, and the tensile strength is considered 10% of the matrix cohesion based on the recommendation by Sainsbury et al. (2008). Implicit joint properties are corresponding to the bedding plane, except the friction is decreased to 24° , and the tensile strength was decreased to 0 MPa. For strain

softening, the critical plastic strain was kept at 0.021% after applying zone size scale correction (Sainsbury and Sainsbury 2017).

The maximum value of total displacement is 26.03 mm, and a total velocity of 0.25 m/s was observed from the numerical analysis. The maximum value of numerical displacement and velocity were observed in the same section on the slope which shows the local instability (Fig. 6a, b). The purpose of numerical simulations was to observe local and global instabilities on the studied slope. The region with a maximum value of numerical velocity and displacement was found to be vulnerable to rockfall events; therefore, the rockfall simulation was also carried out to quantify the risk to the residential buildings located on the opposite side of the road, as shown in Fig. 7a.

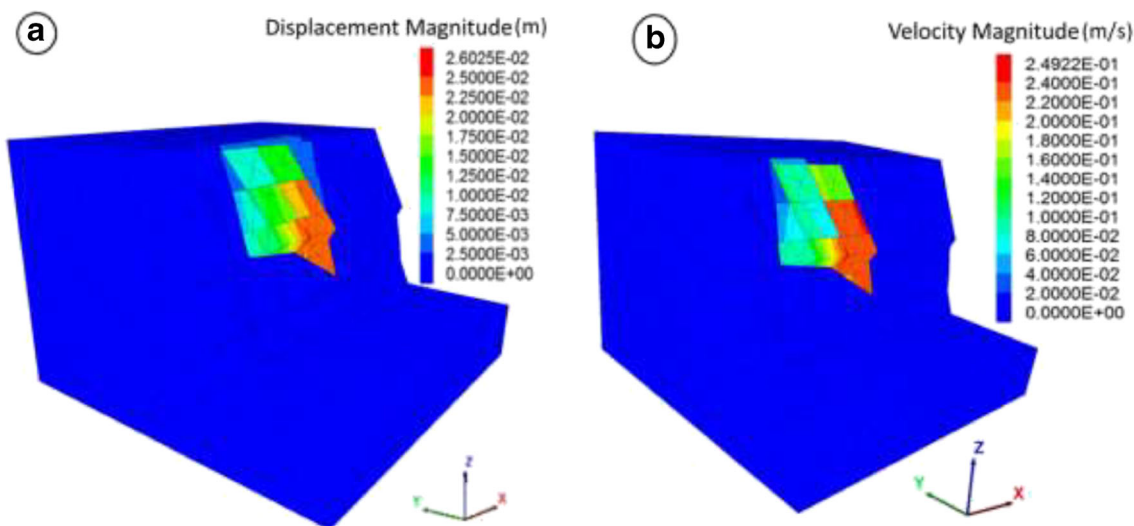


Fig. 6 a Contours of total displacement (in m); b contours of a velocity of blocks (in m/s)

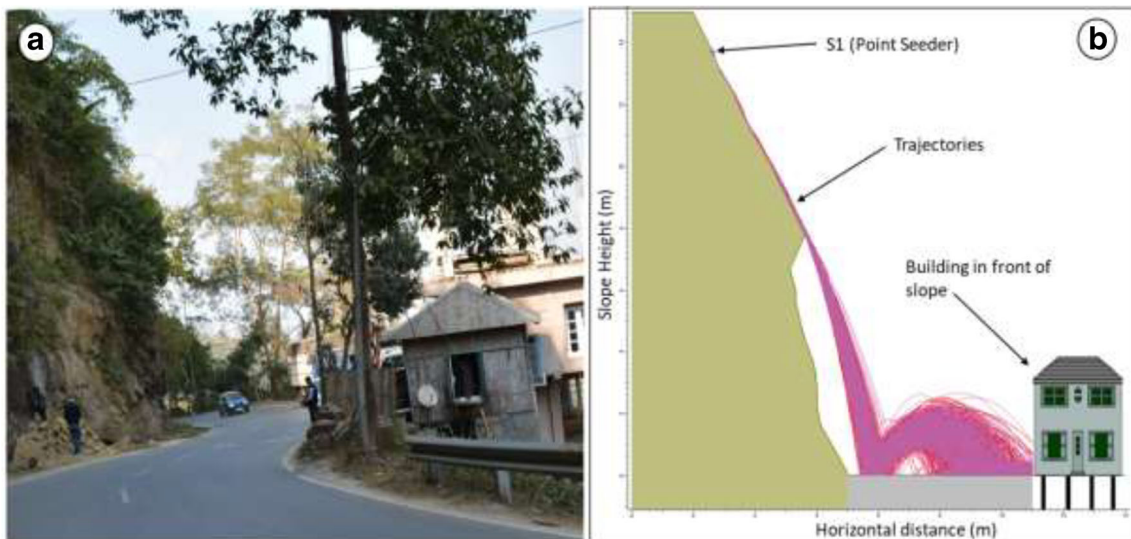


Fig. 7 a Field photograph shows actual slope with houses on the other end; b falling of rock block from the slope surface

Rockfall assessment

Rockfall assessment was carried out on the studied slope to identify the maximum run-out distance, bounce height and the total kinetic energy of the falling rock blocks. The geometry of the slope was prepared in the Rocfall program to represent the actual slope. The model of the slope was divided into two parts, namely, bedrock and roadway. The bedrock consisting of sandstone and asphalt was considered as material for the roadway. The coefficient of restitution (CoR) is one of the important parameters in the rockfall analysis. The value of normal CoR (R_n) was determined in the laboratory, and tangential CoR (R_t) was taken from the CoR table provided by Rocscience (Table 4). The possible trajectory showed that the detached rock block starts with a roll motion, falling from the cliff, and after bouncing on the road, it hit the house in front of the slope (Fig. 7b).

The rockfall initiation position, i.e. seeder point (S1), was considered at the height of 13.7 m from the roadway based on the results of numerical analysis to account for maximum vulnerability. The average mass of 100 kg and 500 kg were assigned to the seeder based on the in situ measurement and numerical simulation. A simulation of 500 trajectories was performed to identify the maximum run-out distance, bounce height and total kinetic energy (KE).

Table 4 Coefficient of restitution table

Colour code	Material	CoR	
		R_n	R_t
	Bedrock (sandstone)	0.45 (± 0.04)	0.85 (± 0.04)
	Asphalt (roadway)	0.4 (± 0.04)	0.9 (± 0.03)

Calculation of normal coefficient of restitution (R_n)

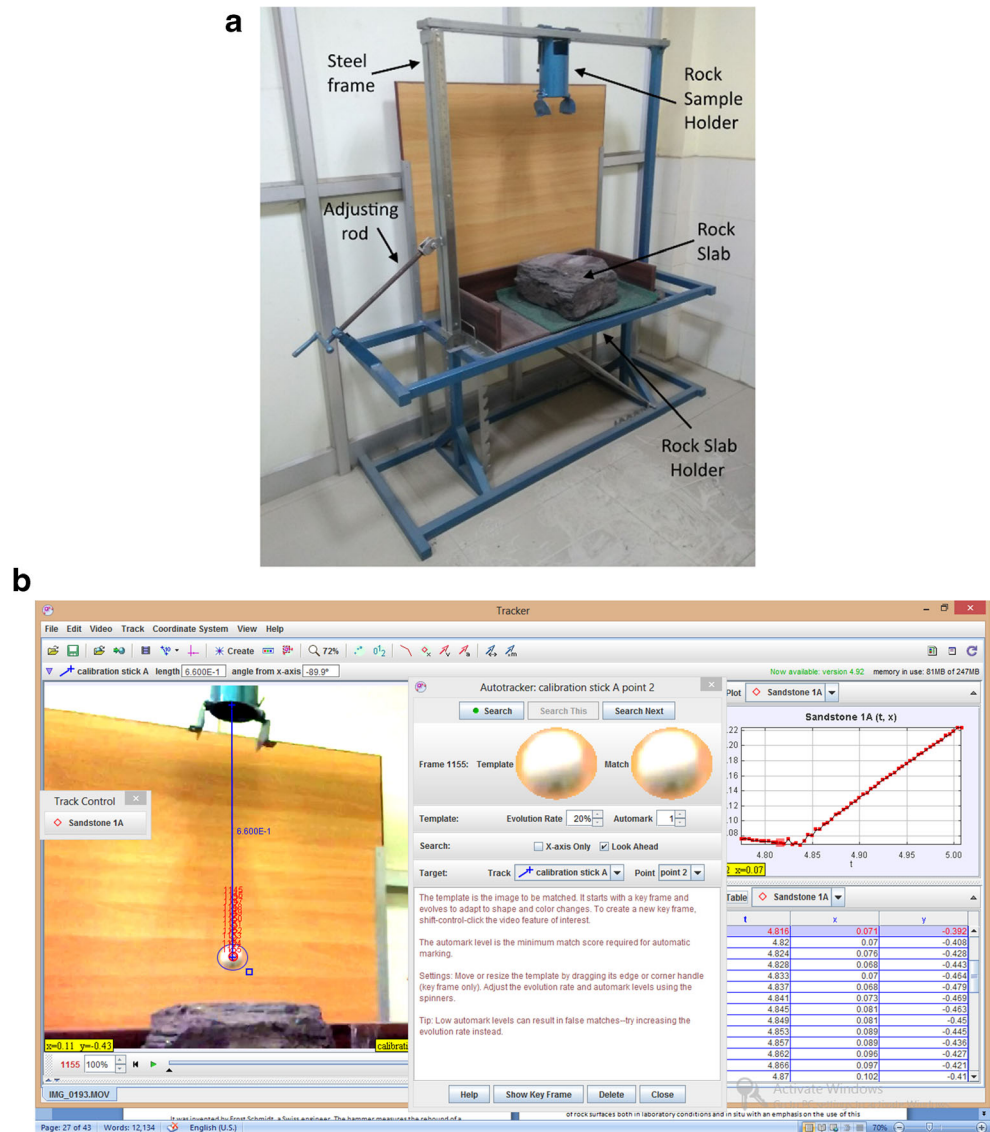
The normal coefficient of restitution (R_n) was determined in the laboratory using a setup, as shown in Fig. 8a (Verma et al. 2019). The setup comprises a steel frame with a sample holder fixed at the top and a rock slab holder at the base. The height of the sample holder and the angle of the resting slab holder can be varied by adjusting the rod and pinion attached to the frame. A high-speed camera was used for image exposures in excess of 1/1000 or frame rates of more than 250 frames per second. It is used to record fast-moving objects as a photographic image(s) onto a storage medium. After recording, the images stored on the medium can be played back in slow-motion. The rock slab was placed on the slab holder at the base of the frame, and a high-speed camera was fixed in front of the setup. The rock sample was held in the sample holder and then released such that it will fall and then bounce on the rock slab. The motion of the block was captured by the camera, and the process was repeated three times. Thereafter, the captured video was analysed using a motion tracking software on the computer (Fig. 8b). The tabulated data were analysed after the required bounce of the sample was tracked in the software. The software generated the velocity variation graph.

The value of R_n was determined using Eq. 3, as given below.

$$R_n = \frac{V_{out}}{V_{in}}, \tag{3}$$

where V_{out} and V_{in} are the velocities of the falling rock block after and before the bounce on the rock slab, respectively, and the experiment was repeated three times, and the average value of R_n was calculated to be 0.45.

Fig. 8 **a** Fabricated experimental setup for CoR; **b** tracking of sample and tabulation of data (Verma et al. 2019)



Bounce height, total kinetic energy and run-out distance

The bounce height is affected by the slope angle, slope surface and shape and size of the rock block. The increase in bounce height was observed, as the detached rock block starts rolling and bouncing on the slope surface. The sudden rise in bounce height occurs at a horizontal distance of 3.25 m due to the falling motion of rock blocks from the slope surface, and as the rock blocks bounce on the roadway, the bounce height again starts to increase and reach the maximum at 2.65 m on the roadway (Fig. 9a).

The potential energy of the rock blocks is converted into kinetic energy as the rock blocks get separated from the slope surface. In the rolling and bouncing motion, kinetic energy increases to 58.58 kJ for a rock block of 500 kg (Fig. 9b).

After falling from the cliff, as the rock blocks hit the roadway, loss of kinetic energy occurs due to the bounce motion of rock blocks. A rock block with this amount of energy can damage a vehicle or disrupt the traffic on the roadway.

The run-out distance helps to find out the maximum reach of falling rock blocks. The analysis reveals that after detached from the slope surface, rock blocks roll and then fall from the surface before bouncing on the road. After bouncing on the highway, 24% rock blocks were observed to be scattered and stopped on the roadway, and the remaining 76% of the rock blocks hit the houses on the other end of the road (Fig. 9c). It was observed that the falling rock blocks make the roadway and residential buildings unsafe for people. The maximum value of bounce height, total kinetic energy and maximum run-out distance observed in the rockfall analysis are reported in Table 5.

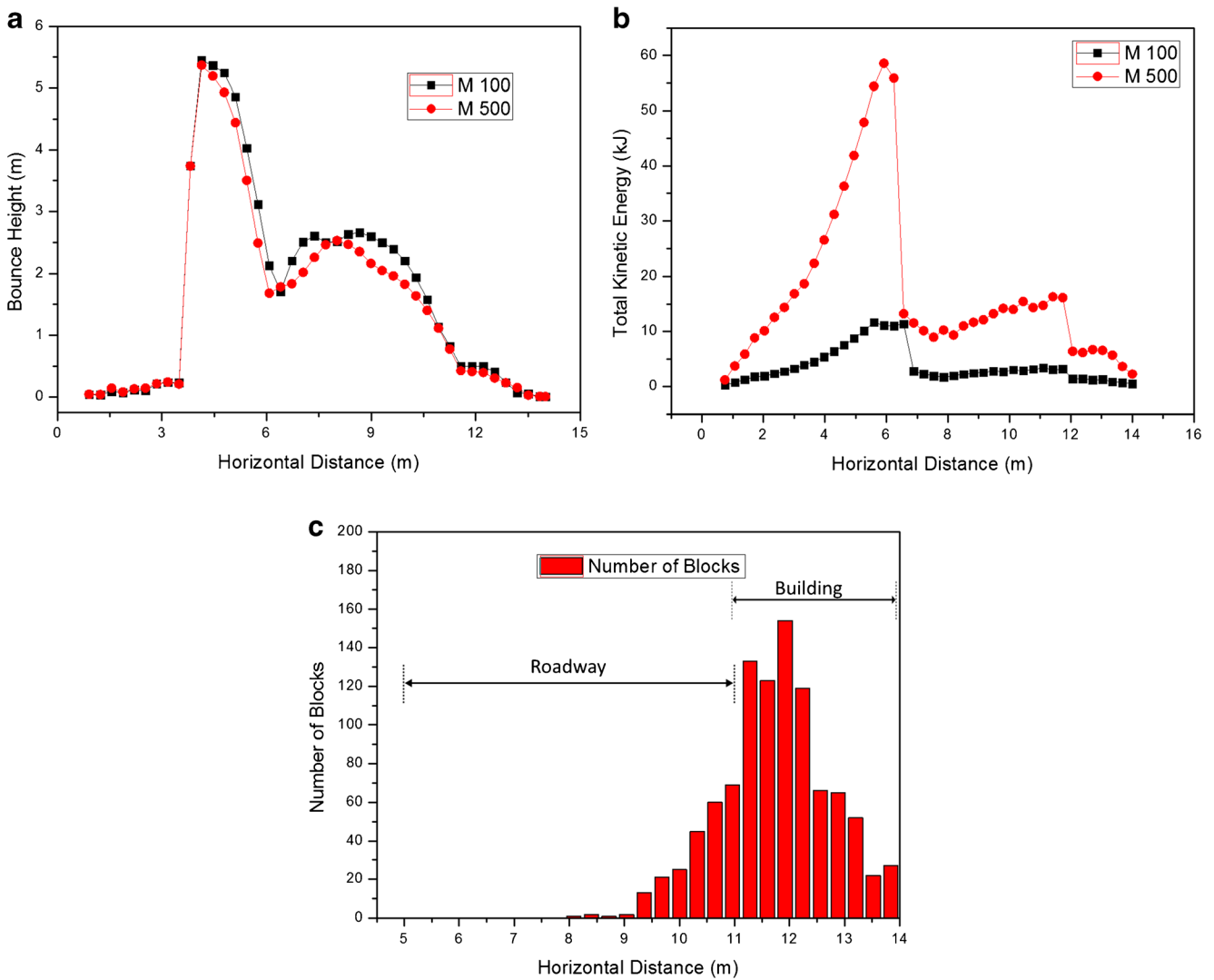


Fig. 9 a Bounce height, b total kinetic energy and c maximum run-out distance of falling rock blocks from the slope

Discussion

The preliminary study conducted by Sardana et al. (2019b) shows that the stability condition of the slope is varying from partial-stable to unstable based on the slope-mass-rating (SMR). The rock mass rating (RMR) classified the studied slope into the fair rockmass classification. Moreover, the slope has a history of rockfall, and the presence of residential area in front of the slope increases the risk factor. Therefore, a detailed stability assessment along the studied slope was necessary.

The results of three-dimensional numerical modelling show that, globally, the slope was stable with a factor of safety 1.1. However, the local slope failure viz. plane and wedge was observed in the slope. The slope with a stretch length of 30 m was simulated to determine the landslide-prone area in front of the buildings located opposite to the slope. The location of the rockfall-prone area on the slope was selected based on the maximum value of numerical velocity and displacement from the numerical modelling results, as shown in Fig. 6. Further, these falling rock blocks have the potential to hit the buildings located on the opposite side of the roadway. Therefore, to

Table 5 Maximum value of output parameters of rockfall analysis on the roadway

Weight (kg)	Maximum bounce height (m)	Total kinetic energy (kJ)	Maximum run-out distance (m)
100	2.65	11.93	14
500	2.52	58.58	14

account for maximum vulnerability, the length of the slope in front of the residential area was considered as a landslide-prone area. Also, the vulnerable section identified in the numerical simulation of the slope is further taken as a rockfall initiation point for the assessment of rockfall.

Rockfall assessment was carried out to quantify the risk associated with the falling rock blocks. Three types of motions, roll, fall, and bounce, were present in the rockfall analysis. After a bounce on the roadway, rock blocks carry the kinetic energy that may hit a vehicle on the roadway and/or destruct houses. The outcome parameters of the rockfall assessment, namely, bounce-height, run-out distance and total kinetic energy reveal that 76% of the simulated rock blocks may hit buildings with a kinetic energy of 58.58 kJ, which makes the roadways and the residential area in front of the slopes unsafe.

Conclusion

3DEC numerical simulation was carried out to understand global and local failures in the jointed road cut slope. Globally, the slope was stable with a factor of safety 1.1; however, local failures, for example, planar and wedge failures, were observed in a certain region of the slope. It was observed that without proper calibration of the joint and matrix properties used in the Ubiquitous-Joint model, the results could be misleading. Ubiquitous-Joint models can provide a robust insight into the deformation and failure process of rockmass at a large scale, which is very difficult using explicit joints due to limited computational power. Unstable sections in the slope are vulnerable to rockfall; therefore, further rockfall analysis was performed.

The safe and unsafe regions on the roadway depend on the maximum distance travelled by the fall-out blocks. The maximum run-out distance of falling rock blocks in rockfall analysis discloses that the whole width of the roadway is unsafe for vehicles, and the residential buildings built on the opposite side to the slope face are under continuous threat. Perret et al. (2004) explain the intensity range based on the kinetic energy of falling rock blocks. The kinetic energies gained by rock blocks of 100 kg and 500 kg are approximately 11.93 kJ and 58.58 kJ, respectively, for this studied slope. The former case makes the slope come under ‘lower intensity ranges’ (< 30 kJ), whereas for the latter case, it comes under ‘medium intensity ranges’ (30–300 kJ). It can be concluded that the bounce height and kinetic energy related to falling rock blocks are enough for the breakdown of vehicles, blockage on the roadway and damages to buildings. The rockfall output parameters can be further used in the selection of appropriate protective measures to make safe living and travelling.

Acknowledgements The authors would like to thank staff of Rock Mechanics Laboratory of IIT (ISM) Dhanbad for their assistance.

Funding MOES (Ministry of Earth Sciences, India) for financially supporting this study (MOES/P.O. (GeoSci)/42/2015).

Compliance with ethical standards

Conflict of interest The authors declare that they have no conflict of interest.

References

- Ansari MK, Ahmad M, Singh R, Singh TN (2016) Rockfall hazard rating system along SH-72: a case study of Poladpur–Mahabaleshwar road (Western India), Maharashtra, India. *Geomatics Nat Hazards Risk* 7(2):649–666
- Barton N (1976) The shear strength of rock and rock joints. *Int J Rock Mech Min Sci Geomech Abstr Pergamon* 13(9):255–279
- Blikra LH, Christiansen HH (2014) A field-based model of permafrost-controlled rockslide deformation in northern Norway. *Geomorphology* 208:34–49
- Cai M, Kaiser PK, Tasaka Y, Minami M (2007) Determination of residual strength parameters of jointed rock masses using the GSI system. *Int J Rock Mech Min Sci* 44(2):247–265
- Chiliza SG, Hingston EDC (2018) Back analysis of an ancient rockslide at Lake Fundudzi, Limpopo Province, South Africa. *Bull Eng Geol Environ* 77(1):29–47
- Ferrari F, Apuani T, Giani GP (2014) Rock mass rating spatial estimation by geostatistical analysis. *Int J Rock Mech Min Sci* 70:162–176
- Itasca (2016) 3DEC - 3 dimensional discrete element code, Version 5.2, User’s manual. Itasca Consulting Group Inc, Minneapolis
- Kesari GK (2011) Geology and mineral resources of Manipur, Mizoram, Nagaland and Tripura. *Geol Surv India* 1:1–103
- Kulhawy FH (1975) Stress deformation properties of rock and rock discontinuities. *Eng Geol* 9(4):327–350
- Kumar N, Verma AK, Sardana S, Sarkar K, Singh TN (2018) Comparative analysis of limit equilibrium and numerical methods for prediction of a landslide. *Bull Eng Geol Environ* 77(2):595–608
- Lallianthanga RK, Lalbiakmawia F (2013) Landslide Hazard zonation of Aizawl district, Mizoram, India using remote sensing and GIS techniques. *Int J Remote Sens Geosci* 2(4):14–22
- Perret S, Dolf F, Kienholz H (2004) Rockfalls into forests: analysis and simulation of rockfall trajectories—considerations with respect to mountainous forests in Switzerland. *Landslides* 1(2):123–130
- Rocscience (2016) RocFall software—for risk analysis of falling rocks on steep slopes. Rocscience Toronto
- Sainsbury BL, Sainsbury DP (2017) Practical use of the ubiquitous-joint constitutive model for the simulation of anisotropic rock masses. *Rock Mech Rock Eng* 50(6):1507–1528
- Sainsbury B, Pierce M, Mas Ivars D (2008) Analysis of caving behaviour using a synthetic rock mass—ubiquitous joint rock mass modelling technique. In *Proceedings of the First Southern Hemisphere International Rock Mechanics Symposium*. Australian Centre for Geomechanics 243–53
- Sardana S, Verma AK, Verma R, Singh TN (2019a) Rock slope stability along road cut of Kulikawn to Saikhamakawn of Aizawl, Mizoram, India. *Nat Hazards* 99(2):753–767
- Sardana S, Verma AK, Singh A, Laldinpuia (2019b) Comparative analysis of rockmass characterization techniques for the stability prediction of road cut slopes along NH-44A, Mizoram, India. *Bull Eng Geol Environ* 78(8):5977–5989
- Sarkar K, Buragohain B, Singh TN (2016) Rock slope stability analysis along NH-44 in Sonapur area, Jaintia hills district, Meghalaya. *J Geol Soc India* 87(3):317–322

- Singh TN, Verma AK (2007) Evaluating the slope instability of the Amiya slide. In 1st Canada-US rock mechanics symposium. American rock mechanics association
- Singh PK, Wasnik AB, Kainthola A, Sazid M, Singh TN (2013) The stability of road cut cliff face along SH-121: a case study. *Nat Hazards* 68(2):497–507
- Tang H, Yong R, Eldin ME (2017) Stability analysis of stratified rock slopes with spatially variable strength parameters: the case of Qianjiangping landslide. *Bull Eng Geol Environ* 76(3):839–853
- Valagussa A, Frattini P, Crosta GB (2014) Earthquake-induced rockfall hazard oning. *Eng Geol* 182:213–225
- Verma AK, Singh TN (2010) Assessment of tunnel instability—a numerical approach. *Arab J Geosci* 3(2):181–192
- Verma AK, Singh TN, Chauhan NK, Sarkar K (2016) A hybrid FEM–ANN approach for slope instability prediction. *J Inst Eng (India) Ser A* 97(3):171–180
- Verma AK, Sardana S, Singh TN, Kumar N (2018) Rockfall analysis and optimized design of rockfall barrier along a strategic road near Solang Valley, Himachal Pradesh, India. *Indian Geotech J* 48(4): 686–699
- Verma AK, Sardana S, Sharma P, Dinpuia L, Singh TN (2019) Investigation of rockfall-prone road cut slope near Lengpui airport, Mizoram, India. *J Rock Mech Geotech Eng* 11(1):146–158
- Wang XL, Zhang LQ, Wang SJ, Agliarid F, Frattini P, Crosta GB, Yang ZF (2012) Field investigation and rockfall hazard zonation at the Shjing Mountains sutra caves cultural heritage (China). *Environ Earth Sci* 66:1897–1908
- Warren SN, Kallu RR, Barnard CK (2016) Correlation of the rock mass rating (RMR) system with the unified soil classification system (USCS): introduction of the weak rock mass rating system (W-RMR). *Rock Mech Rock Eng* 49(11):4507–4518
- Wei LW, Chen H, Lee CF, Huang WK, Lin ML, Chi CC, Lin HH (2014) The mechanism of rockfall disaster: a case study from Badouzh, Keelung, in northern Taiwan. *Eng Geol* 183:116–126
- Wieczorek GF, Jäger S (1996) Triggering mechanisms and depositional rates of postglacial slope-movement processes in the Yosemite Valley, California. *Geomorphology* 15(1):17–31